

An Atomistic Model of the Amorphous Glassy Polycarbonate of 4,4'-Isopropylidenediphenol

M. Hutnik

Department of Materials Science and Engineering, Massachusetts Institute of Technology, Cambridge, Massachusetts 02139

F. T. Gentile,[†] P. J. Ludovice,[‡] and U. W. Suter^{*,§}

Institut für Polymere, ETH-Zürich, CH-8092 Zürich, Switzerland

A. S. Argon

Department of Mechanical Engineering, Massachusetts Institute of Technology, Cambridge, Massachusetts 02139

Received December 31, 1990; Revised Manuscript Received July 1, 1991

ABSTRACT: A detailed static atomistic model of the dense, glassy polycarbonate of 4,4'-isopropylidenediphenol (Bisphenol A polycarbonate (PC)) is simulated by using a well-established technique that previously proved successful for simple vinyl polymers. Initial chain conformations, which are generated by a Monte Carlo technique including periodic continuation conditions, are "relaxed" using a potential energy minimization. Two sizes of microstructures at densities of 1.20 g/cm³ were obtained, one with a cube edge length of 18 Å and the other with an edge length of 30 Å. Detailed analysis of the minimized structures indicates that intermolecular packing effects create a large variation of chain conformations that are different from the purely intramolecular ground states but that it is the intramolecular energy contributions that determine which combinations can or cannot occur. The systems are amorphous, exhibiting random coil behavior, with some weak intermolecular correlations that exist on a very small scale.

I. Introduction

There has been considerable interest in the molecular-level structure of the glassy polycarbonate of 4,4'-isopropylidenediphenol (Bisphenol A polycarbonate (PC)) and its link to bulk mechanical and transport properties. Several investigations have been done by using both experimental¹⁻¹⁵ and theoretical^{9,12,14,16} methods to probe the behavior of glassy PC at the atomistic scale, but whereas the experimental studies have been extensive and precise, the theoretical modeling to date has not been as rigorous, and a detailed molecular-level model of glassy PC is lacking.

Models of amorphous polymers at glass densities with chain backbones less complicated than PC, mainly polyethylene and other vinyl polymers, have been devised using both static^{17,18} and deterministic molecular dynamic (MD)¹⁹⁻²¹ methods and have resulted in varying degrees of success. The extension of these techniques to more complex polymers has been slow. Models of glassy polymers with chain backbones as complex as PC have frequently resorted to gross simplifications of the structure, limiting their application. It was our intent to use a well-established simulation method that has been successful for simple vinyl polymers and extend it to PC. We present here a model of glassy PC using the molecular-static method first developed by Theodorou and Suter for atactic polypropylene¹⁷ (PP) and then modified for atactic poly(vinyl chloride) (PVC) by Ludovice and Suter.¹⁸ It is presently the most detailed model of PC available and has proven very useful in the accompanying atomistic-level

study of conformational alterations of molecular segments of potential importance in mechanical relaxations in PC.²² We shall refer to this study below as III.

II. Previous Work

The molecular-level structure of PC has been well characterized by various experimental techniques, among which are included light scattering,¹ X-ray diffraction,²⁻⁶ and neutron scattering⁷⁻⁹ as well as nuclear magnetic resonance (NMR).¹⁰⁻¹⁵ A brief overview of these studies follows.

Light scattering,¹ small-angle X-ray scattering,² and small-angle neutron scattering^{7,8} studies have shown that single chains of PC in the bulk glass demonstrate random coil behavior. In addition, the wide-angle light scattering analysis of Dettenmaier and Kausch¹ indicates single-phase behavior with no large regions of strong intermolecular orientation correlations. Wide-angle X-ray³⁻⁶ and neutron scattering⁹ have given more detailed insight into the atomistic scale structure of PC. The results of these studies have generally been interpreted as indicating that numerous very small regions of "enhanced order" exist in the bulk, consisting of no more than two or three chemical repeat units. These regions are believed to consist of axially aligned chain segments in which the carbonate group assumes a trans,trans conformation. The regions are too small to alter the overall random coil behavior of the chain or to show large fluctuations in the optical anisotropy of PC.

Various solid-state NMR investigations have been used to probe the atomic-level structure by studying the chain mobility.¹⁰⁻¹⁵ The characteristic chain motions in glassy PC have very broad frequency distributions, indicating large site variations due to differences in intermolecular packing. Henrichs and Nicely¹⁵ also have researched the

[†] Current address: Cellular Transplants, Inc., 4 Richmond Square, Providence, RI 02906.

[‡] Current address: Polygen Corp., 200 Fifth Avenue, Waltham, MA 02254.

[§] Also Department of Chemical Engineering, Massachusetts Institute of Technology, Cambridge, MA 02139.

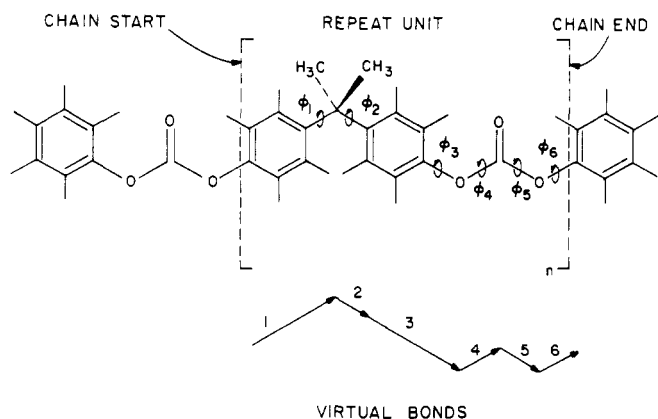


Figure 1. PC repeat unit showing the virtual bonds and their associated torsion angles.

chain conformations of PC in the amorphous bulk and conclude that intramolecular forces largely influence the preferred bulk chain conformations. Specifically, while the phenylene rings widely assume a "propeller" conformation in the isopropylidene moiety of the repeat unit, the carbonate group is oriented out of the plane of its adjacent phenylene rings.

Theoretical modeling specifically on glassy PC has to date been limited. Yannas and Luise¹⁶ developed an early model of glassy PC which includes a molecular-level model that assumes hexagonal packing of quasi-lattice sites with spherical symmetry. The model includes intramolecular interactions represented by intrinsic torsion potentials and intermolecular contribution by Lennard-Jones type interactions between segments. Perchak, Schaefer, and co-workers^{12,14} devised a model consisting of a two-dimensional lattice of interacting phenylene rings with varying degree of lattice flexibility. Fischer et al.⁹ in the analysis of their neutron scattering results modeled PC as "bundles" of parallel segments, two repeat units long. A detailed model of glassy, *bulk* PC has to date been lacking. Previous static^{17,18} and MD^{19–21} simulations done at glass densities have been confined to studying polymers with very simple backbones. MD studies have included models of polyethylene and PP, yet are limited by available computer resources. However, static models of PP by Theodorou and Suter¹⁷ and of PVC by Ludovice and Suter¹⁸ have yielded excellent results while being computationally less intensive than MD simulations. It is our intention here to extend the static simulation technique developed by the aforementioned authors to PC.

III. Generation of Model Structure

1. Model Parameters. The amorphous PC microstructures were generated by the modeling technique developed by Theodorou and Suter¹⁷ for PP and extended to PVC by Ludovice and Suter¹⁸ using the force field described in the previous accompanying paper of this issue,²³ to which we will refer as I. The details of the model are as follows:

A. The model is static, with temperature only entering with the specification of the density at which the structure is relaxed.

B. Spatial periodic continuation conditions are employed for the cubical simulation cell.

C. The bond angles and bond lengths are fixed. Molecular rearrangement occurs only through changing the torsion angles of the bonds (see Figure 1).

D. Methyl groups are represented as pseudoatoms for computational expedience.

E. A Lennard-Jones energy function is used to represent the nonbonded van der Waals interatomic interactions,

while the Coulombic interactions are represented as a Block-Walker function.^{18,24} Intrinsic torsional functions specific to the PC repeat unit are included.²³ Both the Lennard-Jones and the Block-Walker functions are splined due to the finite size of the periodic cube.^{17,18,24}

F. The density is 1.20 g/cm³, appropriate of polycarbonate at room temperature.²⁵

G. Thirteen independent microstructures have been generated with periodic cube edge lengths of 18.44 Å, degree of polymerizations of 35 (MW = 4532), and 485 atoms or atom groups in each cube.

H. Two larger sized microstructures have also been completed, which have periodic cube edge lengths of 29.87 Å, degree of polymerization of 151 (MW = 19 264), and 2051 atoms or atom groups in the cube.

2. Initial Guess. The generation of a starting chain conformation or "initial guess" structure follows the "modified Markov" Monte Carlo process described by Theodorou and Suter¹⁷ with one major alteration. In the original scheme, the chain is generated in a sequential bond-by-bond fashion, where at each step of the generation short-range (via rotational isomeric state (RIS) probabilities²⁶) and long-range interaction energies are included in the weighing of the possible RIS conformations of that bond. For both PP and PVC, the addition of the long-range interactions in the conformational probabilities of the RIS state generated initial guesses that were sufficiently spatially uniform to be readily minimized, even though possible future overlaps of the chain were not anticipated in the generation of the initial guess (the RIS probabilities are bidirectional, but the inclusion of the long-range energy is only unidirectional). While this was not a problem for PP or PVC, it did prove to be significant in the generation of initial guess structures of PC. The energies of the initial guess structures generated by the sequential Monte Carlo scheme were on the order of 10⁸–10¹⁹ kcal/mol, with the majority of the structures in the 10¹¹–10¹² kcal/mol range. The bond segments are much larger and bulkier for PC than for PP or PVC, and therefore the PC chain segments frequently overlapped due to the unidirectionality of the generation technique. The resulting structures were spatially too unevenly distributed, and many could not be minimized. Therefore, the initial guess generation routine was modified. Rather than considering the RIS states of each bond sequentially in the Monte Carlo scheme, a simultaneous choice of the RIS states of the three virtual bonds of the isopropylidene group was made (the bonds labeled 1, 2, and 3 in Figure 1) and included together as one unit; then the conditional probabilities of each possible conformation of the unit as a whole were calculated. The structures generated with the modified routine had energies on the order of 10⁸–10¹² kcal/mol, with the majority of the structures having energies in the range of 10⁸–10¹⁰ kcal/mol. More importantly, the generated structures were more spatially uniform than the structures generated with the unmodified routine. The mean squared end-to-end distances ($\langle r^2 \rangle_0/M$) for 100 generated initial guesses were calculated, with an average of 1.0 ± 0.4 (Å² mol g⁻¹) for degree of polymerization $X = 35$ and an average of 1.2 ± 0.5 (Å² mol g⁻¹) for degree of polymerization $X = 151$. These average values compare well with the experimental range^{7,8,27,28} of 0.75–1.28 (Å² mol g⁻¹) and indicate that the technique correctly generates conformations exhibiting random coil behavior. These initial guess structures were then screened with respect to their energy (taking those of lowest energy) and $\langle r^2 \rangle_0/M$ for minimization.

3. Relaxation to Mechanical Equilibrium. The energy minimization procedure followed the same principles as in the technique developed by Theodorou and Suter.¹⁷ The Eulerian angles (the angles that describe the orientation of the chain with respect to the frame of reference of the cube) and the bond torsion angles (except the first and last along the chain) are considered to be the degrees of freedom for the system. Analytic expressions for the total potential energy with respect to the Eulerian and the rotation angles were derived. A quasi-Newton matrix-updating algorithm due to Broyden, Fletcher, Goldfarb, and Shanno²⁹ was used to minimize the structures. The initial guesses to be minimized were chosen in regards to their energy and so that their average mean squared end-to-end distances agreed well with experimental values. The average $\langle r^2 \rangle_0 / M$ for the smaller cubes was 0.84 ± 0.42 ($\text{\AA}^2 \text{ mol g}^{-1}$) and for the larger cubes was 0.88 ± 0.09 ($\text{\AA}^2 \text{ mol g}^{-1}$).

During the minimization, PC again proved to be much more demanding than PP or PVC. For PP, the initial structures were minimized in three steps using the following modifications to the bonded and nonbonded interactions:

1. The first step included nonbonded forces represented by a soft-sphere function (which only includes the repulsive part of the Lennard-Jones interactions), where the atomic radii were taken at half their actual value. No rotational barriers were included.

2. In the second step, again a soft-sphere function was used, but with atomic radii increased to their actual size. Full rotational barriers were included.

3. For the final step, a full Lennard-Jones function was introduced for the nonbonded interactions with atomic radii taken at their actual size. Full rotational barriers were included.

For PVC, with prominent Coulombic charges, Ludovice and Suter chose a four-step minimization which included the following features:¹⁸

1. The first step employed a soft-sphere function, and the atomic radii and Coulombic charges were taken at half their actual size. No rotational barriers were included.

2. In the second step, a soft-sphere function was used with the atomic radii and Coulombic charges increased to 70% of their actual size. Full rotational barriers were included.

3. A soft-sphere function was again employed for the third step, with the atomic radii and Coulombic charges increased to their actual size and full rotational barriers included.

4. The final step included the full Lennard-Jones function, with the atomic radii and Coulombic charges taken at their actual size and with full rotational barriers.

For PC, it was found that many more steps were necessary, and the minimization was performed in two major stages:

Stage 1: First, using only the soft-sphere function and full rotational barriers, the sizes of the atomic radii were slowly increased (stepwise by 2.5% to 10%) while simultaneously the Coulombic charges were slowly increased to their full values, for an average of 14–20 steps.

Stage 2: Then, with the full Lennard-Jones function and full rotational barriers included, the atomic radii and the Coulombic charges were again slowly increased to their actual sizes, over an average of 13–20 steps.

Overall, more than 25 steps were required in the minimization, which is significantly more than for either PP or PVC. The gradients of energy for PC are also higher than for PP or PVC. For the $X = 35$ microstructures the

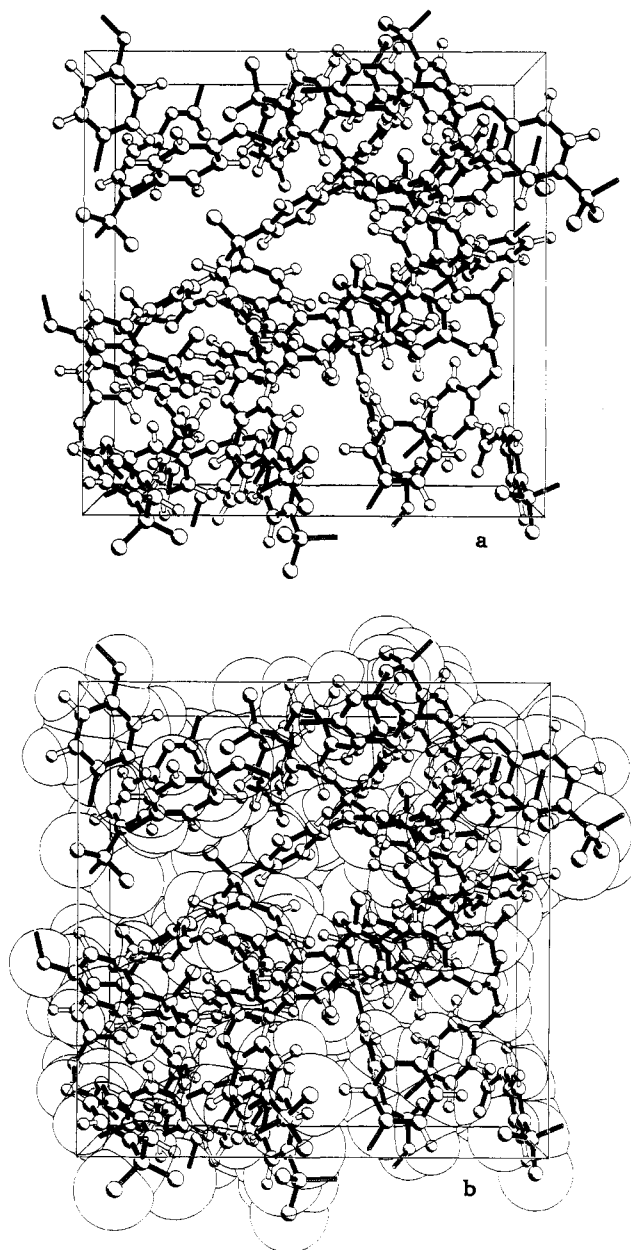


Figure 2. Minimized PC microstructure of $X = 35$. In (a) the atomic radii have been reduced for clarity while in (b) the actual atomic radii have been included.

gradients were less than 10^{-3} kcal/(mol deg), while for the $X = 151$ microstructures they were less than 10^{-1} kcal/(mol deg). The difficulty in the minimization and the higher energy gradients are most likely due to the complexity of the PC repeat unit and the bulkiness associated with the degrees of freedom in the minimization. In Figure 2 a fully minimized structure for $X = 35$ is shown.

This complex minimization procedure brings into question the role of the path dependence of the minimization on the characteristics of the final structures. To investigate this aspect, two different paths were employed. For 6 of the 13 structures with degree of polymerization $X = 35$ that were minimized, the Coulombic charges were included only during the second stage of the minimization. Upon analysis, the two sets of $X = 35$ structures showed no statistical differences from each other, so all 13 were considered as one ensemble.

IV. Results

1. Cohesive Energy Density. The cohesive energy, U_{coh} , is the energy associated only with the intermolecular

Table I
Calculated Energies U_{par} , ΔU_{tails} , and U for PC

	$X = 35$	$X = 151$
$U_{\text{par}},^a$ kcal/(mol of structures)	56.6 ± 16.1	219.3 ± 31.2
$\Delta U_{\text{tails}},^b$ kcal/(mol of structures)	-22.6 ± 2.6	-121.3 ± 6.1
$U,^a$ kcal/(mol of structures)	-260.3 ± 20.1	-1146.5 ± 32.7

^a The range reported is the standard deviation. ^b The effective range for the complete amorphous and for the liquid-like order approximations is reported.

forces and can be estimated from an ensemble of microstructures by taking the difference between the total energy of the microstructure, U_{tot} , and that of the parent chain only, U_{par} . Thus

$$U_{\text{coh}} = U_{\text{par}} - U_{\text{tot}} \quad (1)$$

which relates to Hildebrand's solubility parameter by the following:

$$\delta = (U_{\text{coh}}/V)^{1/2} \quad (2)$$

where V is the volume of the microstructure.

The various energies were determined in a similar manner to the calculations performed on PP¹⁷ and PVC.^{18,24} To determine the parent chain energy of the minimized structures, the cube edge length was increased by 2 orders of magnitude to enclose the chain completely in the box. The energy of this "isolated" chain was then taken as the parent chain energy, U_{par} .

In the calculation of the total energy of the microstructure, U_{tot} , since the nonbonded energy interactions had been splined in the minimization, a "tail correction" factor had to be introduced. With the inclusion of the Coulombic interactions, the tail correction calculation becomes quite complex, leading to upper and lower bounds for the tail correction where the lower bound is achieved by assuming the structure is completely amorphous and the upper bound is calculated by assuming liquid-like ordering of the dipoles.^{18,23,24}

Overall, the cohesive energy becomes

$$U_{\text{coh}} = U_{\text{par}} - U_{\text{tot}} = U_{\text{par}} - [U + \Delta U_{\text{tails}}] \quad (3)$$

where U is the total energy of the microstructure and ΔU_{tails} is the tail correction. Table I lists the calculated energies for the thirteen 18-Å cubic structures (degree of polymerization $X = 35$) and for the two 30-Å cubic structures (degree of polymerization $X = 151$). Thus we obtain the following ranges for the Hildebrand solubility parameters δ (limits are standard deviations):

$$\delta = 19.4 \pm 1.1 \text{ (J/cm}^3\text{)}^{1/2} \quad (13 \text{ structures, } X = 35) \quad (4a)$$

$$\delta = 19.7 \pm 0.5 \text{ (J/cm}^3\text{)}^{1/2} \quad (2 \text{ structures, } X = 151) \quad (4b)$$

The reported experimental values for the solubility parameter for PC are 20.3 and 20.1 $\text{(J/cm}^3\text{)}^{1/2}$.^{30,31} Hence, the theoretical predictions provide quite reasonable results.

2. Conformation of the Individual Chains in Bulk.

There are several aspects of the individual chain behavior in the bulk that can be investigated with the model and compared with experiment. The first of these is the random coil behavior. As previously stated, in the initial guess generation the chain conformations demonstrate random coil statistics. As with PP and PVC, the $\langle r^2 \rangle_0/M$ of the overall chain conformation in the microstructures does not dramatically change during minimization.^{17,18} For the fully minimized structures, the average $\langle r^2 \rangle_0/M$ for

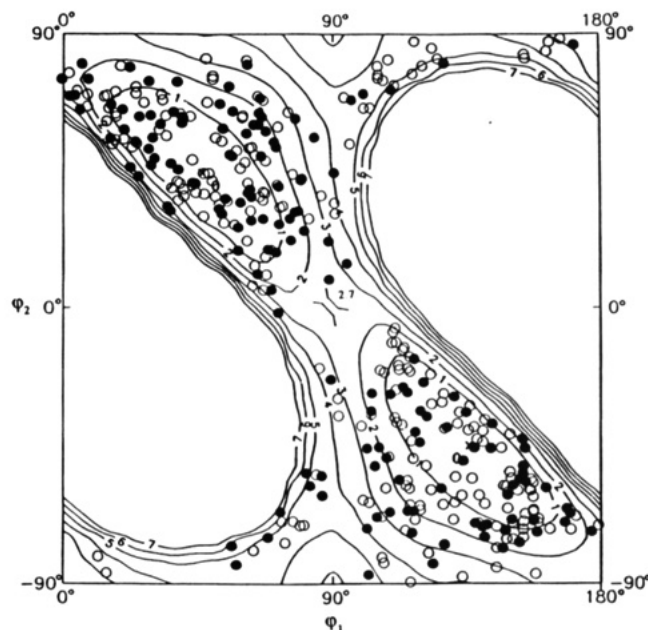


Figure 3. Intramolecular vs intermolecular influence of the phenylene ring conformations in the isopropylidene group. The background is a contour map of ϕ_1 vs ϕ_2 computed using 2,2-diphenylpropane,²³ with 'x's located at $(45^\circ, 45^\circ)$ and at $(135^\circ, -45^\circ)$ representing the ground states or RIS conformations. The energy contour levels indicate incremental increases of 1 kcal/mol above the ground states. Overlaid on the contour map are the values of the torsion angles occurring in the 15 microstructures. The open circles are the conformations existing in the $X = 35$ microstructures, and the filled circles are the conformations existing in the $X = 151$ microstructures.

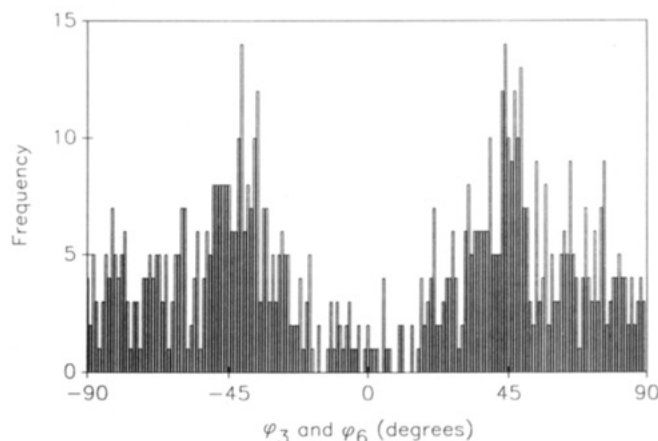


Figure 4. Distribution of torsion angles occurring in the 15 microstructures. The intramolecular ground states or RIS conformations are located at about $+45^\circ$ and -45° and are equally populated in the initial guess structures.

the $X = 35$ microstructures is (standard deviation in parentheses) $0.96 (\pm 0.40) \text{ \AA}^2 \text{ mol}^{-1}$ and for the $X = 151$ microstructures the average is $0.90 (\pm 0.14) \text{ \AA}^2 \text{ mol}^{-1}$, which again compare well with the reported experimental range of 0.75–1.28.^{7,8,27,28}

Another important area to investigate is the influence of intermolecular packing on the chain conformation with respect to the intramolecular ground-state conformations of the isolated molecule. NMR studies show that site inhomogeneity due to intermolecular packing must exist, while at the same time intramolecular forces dominate the preferred bulk chain conformations.^{10–15} These at first seemingly contradictory findings are supported in our model. Figures 3–5 reveal the effects of intermolecular packing on the conformations of the individual torsion

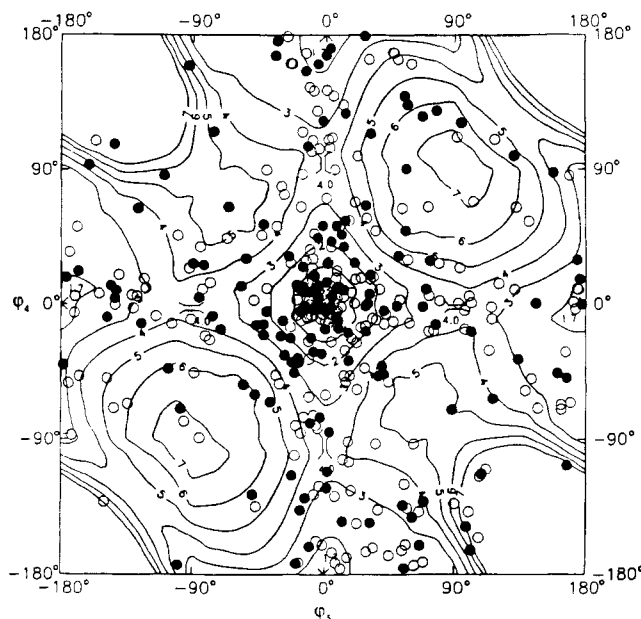


Figure 5. Intramolecular vs Intermolecular influence for the carbonate group conformations. The background is a contour map of torsion angles φ_4 vs φ_5 calculated using diphenyl carbonate.²³ The ground states, located at $(0^\circ, 0^\circ)$ for the trans,trans conformation and at $(0^\circ, 180^\circ)$, $(0^\circ, -180^\circ)$, $(-180^\circ, 0^\circ)$, and $(180^\circ, 0^\circ)$ for the trans,cis and cis,trans conformations, are indicated with x's. The energy contour levels indicate incremental increases of 1 kcal/mol above the trans,trans conformation. Overlaid on the contour map are the carbonate conformations that occur in the 15 microstructures. The open circles are the conformations existing in the $X = 35$ microstructures, and the filled circles are the conformations existing in the $X = 151$ microstructures.

angles. In the PC repeat unit (see Figure 1), the conformations can be grouped into three types:

1. For the two torsion angles φ_1 and φ_2 which determine the rotation of the phenylene rings with respect to the isopropylidene group, the intramolecular ground state, determined through calculations done on 2,2-diphenylpropane, occurs when the phenylene rings are rotated out of the plane in a "propeller-like" conformation. The results discussed in I show that the rotation of the two angles is highly interdependent.²³

2. The two torsion angles φ_3 and φ_6 indicate the conformation of the phenylene rings with respect to the carbonate group that they bracket. Using diphenyl carbonate as a model compound shows that the intramolecular ground states for these torsion angles are not highly interdependent and occur when the phenylene rings are rotated out of the plane of the carbonate group by about 45° .²³

3. Finally, φ_4 and φ_5 determine the conformation of the carbonate group locally. Using diphenyl carbonate as a model reveals that the ground intramolecular energy states exist when the carbonate group is in its trans,trans state, with additional minima in the cis,trans or trans,cis states.²³ The rotation of these two angles exhibits a strong interdependency.

During the analysis, no visible difference could be seen between the conformations of the 18-Å cube vs the 30-Å cube, so the compilation of the individual torsion angle conformations of all 15 microstructures together is compared with the intramolecular ground states and RIS states in Figures 3–5. In Figure 3, the background is a contour map of φ_1 vs φ_2 computed using 2,2-diphenylpropane, with x's located at $(45^\circ, 45^\circ)$ and at $(135^\circ, -45^\circ)$ representing equivalent ground-state or RIS conformations. The energy

contour levels indicate incremental increases of 1 kcal/mol above the ground states. Overlaid on the contour map are the values of the torsion angles that exist in the 15 microstructures. The open circles are the conformations existing in the $X = 35$ microstructures, and the filled circles are the conformations existing in the $X = 151$ microstructures. Upon inspection, it is obvious that the torsion angles are not in their lowest energy conformations and that there exists a large variation of behaviors. However, the large majority of the torsion angles occur in troughs of low intramolecular energy clustering around the ground state. No conformations exist with intramolecular energies above about 7 kcal/mol. This indicates that, for the torsion angles in the isopropylidene group, the intermolecular packing effects create a large variation of torsion angle combinations, but it is the intramolecular energy contributions that determine the reference contour combinations which can or cannot occur, in broad agreement with NMR studies.^{10–15}

For torsion angles φ_3 and φ_6 , these two angles are not closely interdependent, so the analysis can be presented as a bar graph. In Figure 4, the individual torsion angle conformations occurring in the 15 microstructures are represented as "Dirac pulses". The intramolecular ground states or RIS conformations are located at about $+45^\circ$ and -45° out of the plane of the carbonate group. The figure shows that again the conformations occurring in the bulk are varied but are nonetheless centered around the intramolecular ground states. This is in agreement with the finding of Henrichs and Nicely that the phenylene rings are rotated out of the plane of the carbonate group in the bulk.¹⁵ The intramolecular energy barriers for these torsion angles are much less steep than the contours that occur in the isopropylidene group and therefore show more scatter.

This large scatter of torsion angle values becomes even more apparent when the conformations of the carbonate group, φ_4 and φ_5 , are studied. In Figure 5 the background is a contour map of torsion angles φ_4 vs φ_5 calculated using diphenyl carbonate. The energy contour levels indicate incremental increases of 1 kcal/mol above the trans,trans conformation. The ground states indicated with x's are located at $(0^\circ, 0^\circ)$ for the trans,trans conformation and at $(0^\circ, 180^\circ)$, $(0^\circ, -180^\circ)$, $(-180^\circ, 0^\circ)$, and $(180^\circ, 0^\circ)$ for the trans,cis and cis,trans conformations. The carbonate group is much "softer" than the isopropylidene group, resulting in larger areas of low energy and less steep energy well walls. Overlaid on the contour map are the carbonate conformations existing in the 15 microstructures. Again, the open circles are the conformations existing in the $X = 35$ microstructures, and the filled circles are the conformations existing in the $X = 151$ microstructures. Immediately we see that the large majority of the carbonate groups are not planar and that there is a wide scatter of conformations, including several with quite high intramolecular energies. The presence of the high intramolecular energy conformations of the carbonate group indicates that the intermolecular packing influences the conformation of the carbonate group more than for the phenylene rings, which are more dominated by intramolecular forces.

3. Structure of the Glassy Polymeric Bulk. Structural detail of the intermolecular packing can be gained by using the "bond direction correlation function",³² which is used to measure the orientation correlation between

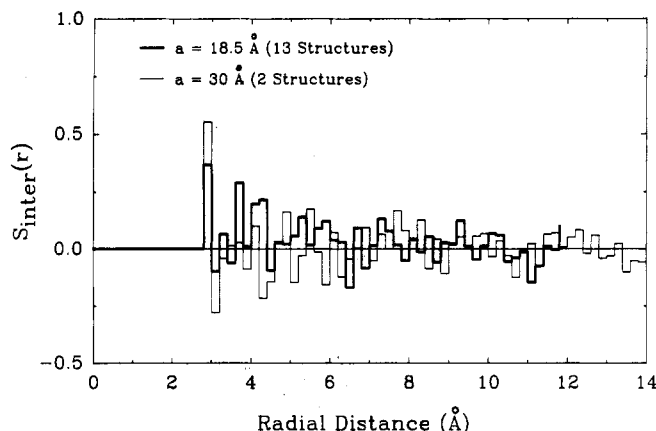


Figure 6. Intermolecular average bond direction correlation function $S_{\text{inter}}(r)$ calculated for the carbonate groups.

bonds. The function is described by the equation

$$S_{ij} = [3\langle \cos^2 \Theta_{ij} \rangle - 1]/2 \quad (5)$$

where Θ_{ij} is the angle along the chain between two segments (bond chords) of a chain. The intermolecular correlation function, $S_{\text{inter}}(r)$, is obtained by averaging over segments of different images of the parent chain with a given distance r between chord midpoints. It indicates the frequency of various intermolecular correlations at given distances: positive values indicate a tendency of parallel alignment of the segments, while negative values reflect a tendency toward perpendicular alignment. For PC, $S_{\text{inter}}(r)$ was calculated for the carbonate groups and is shown in Figure 6. It should be noted that, for calculations based upon the sum of pairwise interactions, there are many more pairs in one of the $X = 151$ microstructures than in one of the $X = 35$ microstructures, so the calculations done on the two larger systems are comparable to calculations done on the sum of the thirteen smaller systems. Upon inspection of Figure 6, one sees that there is a tendency toward parallel alignment at a distance of approximately 3 Å. This is the first indication that there is some trace of weak intermolecular order in the PC microstructures, albeit quite weak.

Atomic pair distribution functions can further elaborate the intermolecular structure. Pair correlation functions, $g_{ij}(r)$, were calculated for all possible pairs. This function is defined by equating $(4\pi/V)g_{ij}(r)r^2 dr$ to the probability of finding an i atom and a j atom at a distance between r and $r + dr$, where V is the volume of one microstructure. For PC, there exist 9 different types of atoms^{23,33} when the methyl group atoms are treated explicitly, which therefore yield 45 distinct pairs of atoms. The total $g_{ij}(r)$ for each pair is the sum of intramolecular and intermolecular contributions, where the intramolecular contribution is obtained by "blowing up" the cube to such a degree to isolate the parent chain and thus count only the interactions belonging to the same chain. The intermolecular contribution is then the difference between the total and the intramolecular $g_{ij}(r)$. Since not all of the 45 plots can be shown here, only those cases where interesting structural information can be seen are featured. The two sizes of microstructures are treated separately. Although there are some visible small differences based on cube size, no trends can be detected.

In the first atomic pair distribution function, hydrogen-hydrogen (H-H) (Figure 7),³³ the functions of both sizes of cubes quickly level off to unity, showing that there is no correlation of structure with respect to hydrogen atoms. The next pair distribution function to be presented is the

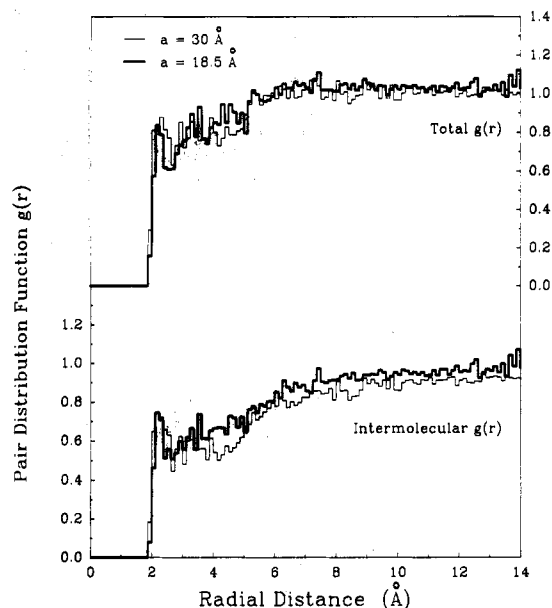


Figure 7. Hydrogen-hydrogen (H-H) atomic pair distribution function.

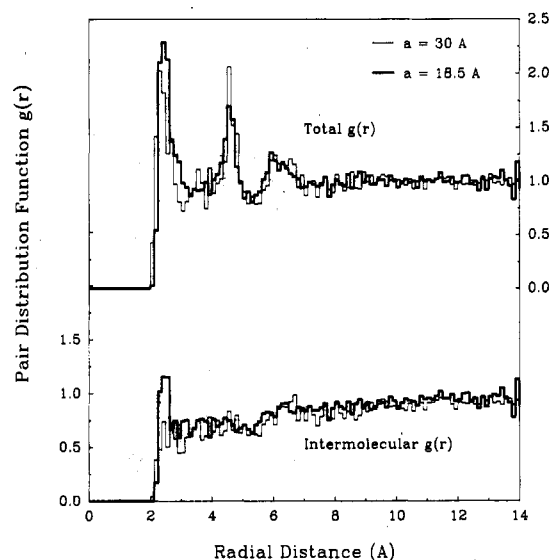


Figure 8. Carbonate oxygen-hydrogen (O-C=O-H) atomic pair distribution function.

carbonyl oxygen-hydrogen (O-C=O-H) pair and can be seen in Figure 8. As expected, there exists a strong intramolecular correlation due to the hydrogens on the phenylene rings flanking the carbonate group, but once the intramolecular contribution is removed, no significant correlation is found. The main-chain oxygen-hydrogen (O-H) distribution, which is not shown here, demonstrates the same amorphous behavior.

Some of the pair distribution functions do show some intermolecular correlations. The isopropylidene carbon-isopropylidene carbon ($C^{\text{al}}-C^{\text{al}}$), the carbonate carbon-carbonate carbon ($C^{\text{C=O}}-C^{\text{C=O}}$), the carbonate carbon-carbonate oxygen ($C^{\text{C=O}}-O^{\text{C=O}}$), and the carbonate carbon-main-chain oxygen ($C^{\text{C=O}}-O^{\text{main}}$) pair distribution functions, featured respectively in Figures 9–12, all show some intermolecular correlations in both sizes of microstructures. These correlations are not particularly strong but do suggest that some areas of the structure are not strictly amorphous, as was the case with PP.¹⁷ The correlations found in the $C^{\text{al}}-C^{\text{al}}$ pair distribution function, shown in Figure 8, indicate that there is some weak intermolecular preference for distances of about 5–6 Å, which could be

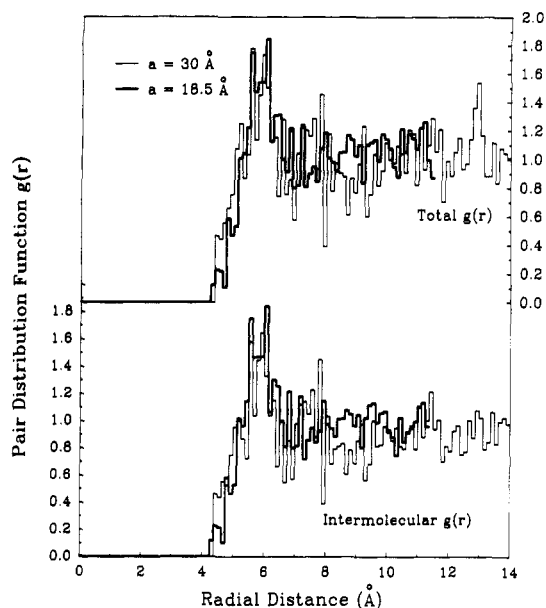


Figure 9. Isopropylidene carbon-isopropylidene carbon ($C^{al}-C^{al}$) atomic pair distribution function.

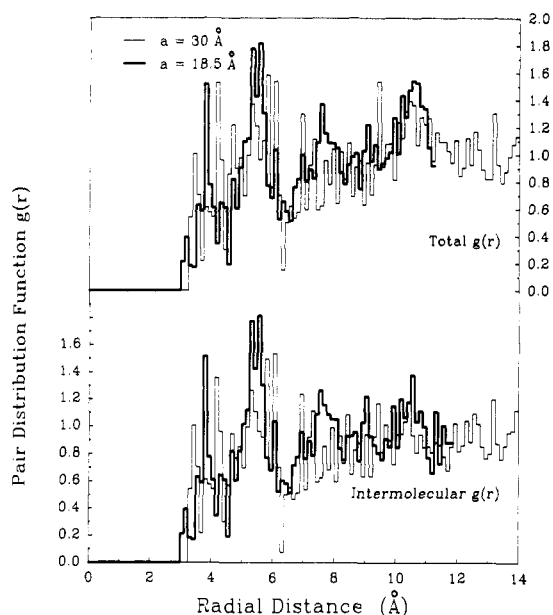


Figure 10. Carbonate carbon-carbonate carbon ($C^{O}-C^{O}$) atomic pair distribution function.

an indication of the areas of "enhanced order" found using experimental wide-angle scattering techniques.^{3-6,9}

Other structural features were also examined. The spatial uniformity of the structures was studied and indicated that there are some "large" inhomogeneities in PC in the form of empty space in the box on the order of 3–5 Å in diameter. A more rigorous analysis of the empty space was performed by Arizzi and Suter³⁴ and demonstrated that the degree of heterogeneity in PC was not a function of the cube size. This feature along with the other analysis presented here shows few differences between the two sizes of microstructures indicating that the system is already "converged" at the smaller cube size and that both sizes can be used for future simulations of the structural detail of PC.

V. Conclusions

The analysis of the PC microstructures shows that the PC chain exhibits random coil behavior in the bulk. Both

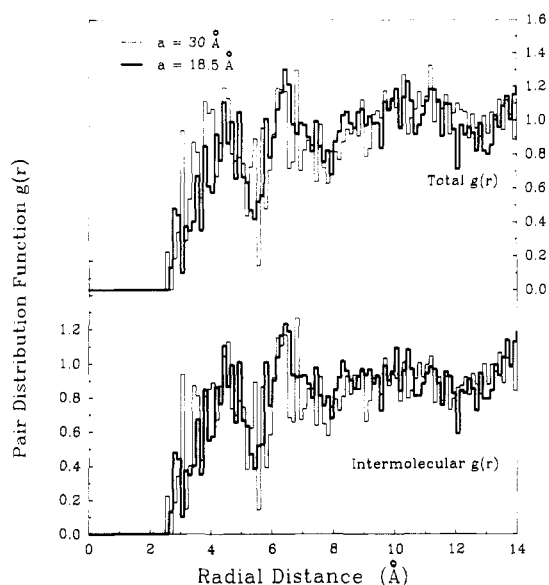


Figure 11. Carbonate carbon-carbonate oxygen ($C^{O}-O-C^{O}$) atomic pair distribution function.

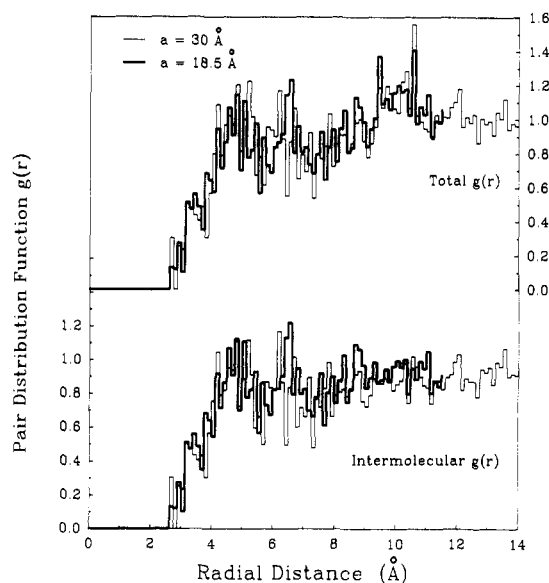


Figure 12. Carbonate carbon-main-chain oxygen ($C^{O}-O$) atomic pair distribution function.

the intramolecular and intermolecular contributions determine the individual chain conformations, with the intramolecular forces dictating which conformations are possible and which are not. The intermolecular forces, especially for the carbonate group, contribute to the large variation of conformations that are centered around the intramolecular ground states. On the whole, the structure of PC is amorphous, although some weak intermolecular correlations on a very small scale do exist. The features studied show excellent agreement with experiment, indicating good quality of the simulated PC microstructures and their usefulness for future simulations.

Acknowledgment. This research was supported by the Defense Advanced Research Projects Agency through the Office of Naval Research under Contract N00014-86-K-0768. M.H. is a member of the Program in Polymer Science and Technology at MIT. We thank P. H. Mott and M. F. Sylvester for many helpful discussions.

References and Notes

- (1) Dettenmaier, M.; Kausch, H. H. *Colloid Polym. Sci.* **1981**, *259*, 209.

- (2) Wendorff, J. H.; Fischer, E. W. *Kolloid-Z. Z. Polym.* **1973**, *251*, 876.
- (3) Wignall, G. D.; Longman, G. W. *J. Mater. Sci.* **1973**, *8*, 1439.
- (4) Turska, E.; Hurek, J.; Zmudzinski, L. *Polymer* **1979**, *20*, 321.
- (5) Mitchell, G. R.; Windle, A. H. *Colloid Polym. Sci.* **1985**, *263*, 280.
- (6) Schubach, H. R.; Heise, B. *Colloid Polym. Sci.* **1986**, *264*, 335.
- (7) Ballard, D. G. H.; Burgess, A. N.; Cheshire, P.; Janke, E. W.; Nevin, A.; Schelten, J. *Polymer* **1981**, *22*, 1353.
- (8) Gawrisch, W.; Brereton, M. G.; Fischer, E. W. *Polym. Bull.* **1981**, *4*, 687.
- (9) Cervinka, L.; Fischer, E. W.; Hahn, K.; Jiang, B.-Z.; Hellman, G. P.; Kuhn, K.-J. *Polymer* **1987**, *28*, 1287.
- (10) Spiess, H. W. *Advances in Polymer Science*; Kausch, H. H., Zachmann, H.-G., Eds.; Springer-Verlag: Berlin, 1984.
- (11) Roy, A. K.; Jones, A. A.; Inglefield, P. T. *Macromolecules* **1986**, *19*, 1356.
- (12) Perchak, D.; Skolnick, J.; Yaris, R. *Macromolecules* **1987**, *20*, 121.
- (13) Ngai, K. L.; Rendell, R. W.; Yee, A. F. *Macromolecules* **1988**, *21*, 3396.
- (14) Walton, J. H.; Lizak, M. J.; Conradi, M. S.; Gullion, T.; Schaefer, J. *Macromolecules* **1990**, *23*, 416.
- (15) Henrichs, P. M.; Nicely, V. A. *Macromolecules* **1990**, *23*, 3193.
- (16) Yannas, I. V.; Luise, R. R. *J. Macromol. Sci., Phys.* **1982**, *B21* (3), 443.
- (17) Theodorou, D. N.; Suter, U. W. *Macromolecules* **1985**, *18*, 1467.
- (18) Ludovice, P. J.; Suter, U. W. "Detailed Molecular Structure of a Polar Polymer Glass", manuscript submitted for publication.
- (19) Clarke, J. H. R.; Brown, D. *Mol. Sim.* **1989**, *3*, 27.
- (20) Ludovice, P. J.; Suter, U. W. *Polym. Prepr. (Am. Chem. Soc., Div. Polym. Chem.)* **1989**, *30*, 14.
- (21) Sylvester, M. F.; Yip, S.; Argon, A. S. *Polym. Prepr. (Am. Chem. Soc., Div. Polym. Chem.)* **1989**, *30*, 32.
- (22) Hutnik, M.; Argon, A. S.; Suter, U. W. *Macromolecules*, following paper in this issue.
- (23) Hutnik, M.; Argon, A. S.; Suter, U. W. *Macromolecules*, previous paper in this issue.
- (24) There is one difference in the treatment of the Coulombic charges for PVC vs PC. The electrostatic nonbonded interactions are represented by the following Coulomb potential:

$$U_{ij}^C(r) = \frac{1}{4\pi D(r)\epsilon_0} \left(\frac{q_i q_j}{r} \right) \quad (\text{i})$$

where U_{ij}^C is the electrostatic pairwise interaction potential, ϵ_0 is the permittivity in a vacuum, $D(r)$ is the effective dielectric

constant, and the q 's are the partial charges on atoms i and j .^{18,23} A distance-dependent dielectric constant $D(r)$ is used, based on the following approximation:

$$D(r) = 1 \quad \text{for } r < a \quad (\text{ii})$$

$$D(r) = \epsilon_B \exp(-\kappa/r) \quad \text{for } r > a \quad (\text{iii})$$

$$\kappa = a \ln(\epsilon_B) \quad (\text{iv})$$

where ϵ_B is the dielectric constant of the bulk polymer. The radial distance a at which D switches from unity to an exponentially decaying function is chosen to be the same for all atom pairs and is the sum of the smallest and the largest van der Waals radii for the charged atoms. The choice of a made for PC differs from that made in the calculations of Ludovice and Suter,¹⁸ where a was allowed to vary according to the sum of the van der Waals radii of atoms i and j . In the spline and the tail correction calculations a fixed value of a is used, which simplifies the calculations considerably.

- (25) From the chapter "Polycarbonates" in the *Encyclopedia of Polymer Science and Engineering*, 2nd ed.; John Wiley and Sons, Inc.: New York, 1988; Vol. 11, p 656.
- (26) Flory, P. J. *Statistical Mechanics of Chain Molecules*, reprinted edition; Oxford University Press: New York, 1988.
- (27) Berry, G. C. *J. Chem. Phys.* **1967**, *46*, 1338.
- (28) de Chirico, A. *Chim. Ind.* **1960**, *42*, 248.
- (29) Hillstom, K. "Nonlinear Optimization Routines in AMBLIB", Technical Memorandum No. 297, Argonne National Laboratory, Applied Mathematics Division, 1976.
- (30) Van Krevelan, D. W.; Hoftyzer, P. J. *Properties of Polymers: Their Estimation and Correlation with Chemical Structure*; Elsevier: New York, 1976; pp 130, 137, 275.
- (31) Bayer, AG, Leverkusen, FRG, private communication.
- (32) Weber, T. A.; Helfand, E. *J. Chem. Phys.* **1979**, *71*, 4760. Dill, K. A.; Flory, P. J. *Proc. Natl. Acad. Sci. U.S.A.* **1980**, *77*, 3115. Vacatello, M.; Avitabile, G.; Corradini, P.; Tuzi, A. *J. Chem. Phys.* **1980**, *73*, 543.
- (33) Methyl hydrogens have been placed on the methyl groups in a staggered conformation for the pair distribution function calculations since for the minimization the methyl groups were represented as pseudoatoms.
- (34) Arizzi, S.; Suter, U. W., manuscript to be submitted.

Registry No. PC (copolymer), 25037-45-0; PC (SRU), 24936-68-3.